

Механика на твърдото деформируемо тяло

Numerical determination of plastic localization during extrusion of metals

N. Bontcheva

1. Introduction

Plastic localization during metal forming processes creates conditions for development of structural changes, crack initiation, etc. and hence affects the final production. The plastic localization zone during extrusion is built at the very beginning when the process is unsteady. When the steady process takes place, the metal flows along the existing dead zone.

As plastic strains during metal forming processes are much larger compared with the elastic ones, the latter are neglected and the rigid-plastic model is assumed. In the case of a perfectly plastic body and neglecting thermal effects, the basic system of equations describing the process is hyperbolic and the method of characteristics is used for solving it [1]. The large plastic strains cause energy dissipation and heat production which causes increasing of temperature, especially in the plastic localization zones. The yield limit is sensitive to temperature and decreases considerably. This makes necessary the investigation of the coupled thermomechanical problem.

The extrusion of metals, neglecting thermal effects is considered in [2, 3, 4, 9]. In [4,5] the extrusion of thermo-elastic-plastic bodies is investigated. In [6, 7, 8] viscoplastic materials are considered. The numerical method, given in [10] will be applied here for simulating the extrusion of a rigid-plastic hardening, rate-sensitive and temperature-sensitive material. The method is based on a combination of the finite-element method with the free-point-method and is suitable for solving unsteady problems. The program system TFARM, mentioned in [10] will be used.

2. The Boundary value problem

Consider the two-dimensional problem of plane and axisymmetric extrusion (fig. 1). The relation

$$(2.1) \quad |\varepsilon| = 1 - \left(\frac{R_2}{R_1}\right)^2$$

defines the reduction degree. Oz is the symmetry axis. Initially the material occupies the region $ABCDE$. As soon as the piston AB starts to move forward, the material flows out of the opening ED and the region $EDFE'$ gets larger (fig. 1 b). There exists friction along the sides BC and CD . Siebel's friction law is assumed, $0 \leq m \leq 1$ being

the friction factor. Due to the symmetry the transversal, resp. the radial velocity vanishes along AE and CEE' : $v_r = 0$. Along the walls the following conditions are fulfilled:

$$(2.2) \quad \begin{aligned} v_r &= 0 \text{ at } BC \\ v_z &= 0 \text{ at } CD, \end{aligned}$$

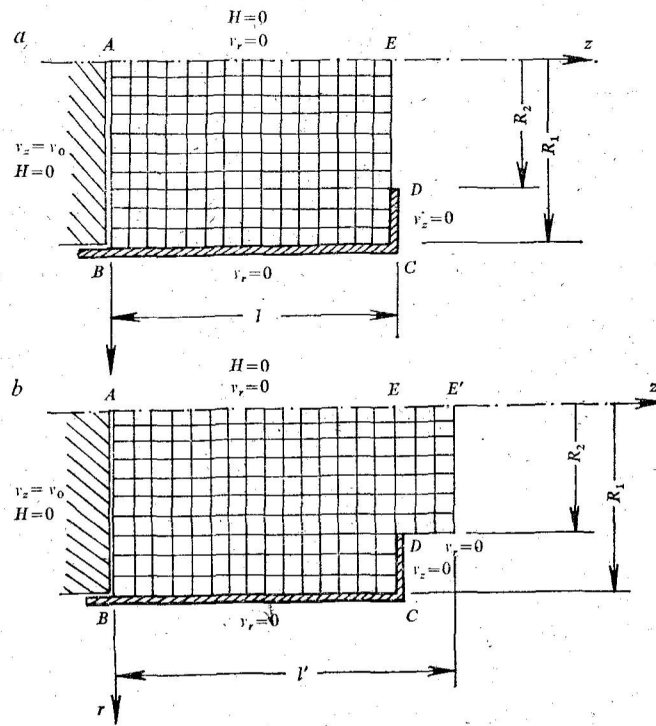


Fig. 1

The velocity of the piston AB is prescribed:

$$(2.3) \quad v_z = v_0 \text{ at } AB.$$

The initial temperature of the material is given:

$$(2.4) \quad T(r, z, 0) = T_0(r, z).$$

Heat exchange with the surroundings takes place during the process along DE resp. along DEE' , according to the law

$$(2.5) \quad \frac{\partial T}{\partial n} = -\frac{H}{\lambda} [T(r, z, t) - T_{\text{ref}}(t)],$$

where H is the heat transfer coefficient, λ is the heat conductivity, T_{ref} is the temperature of the surrounding medium. At BC and CD heat transfer through the walls takes place. According to [11, 10] we assume that the boundary condition there has also the form (2.5) but the coefficient H is calculated by means of the thickness of the wall and the surface of heat transfer.

At the symmetry axis the condition

$$(2.6) \quad \frac{\partial T}{\partial n} = 0$$

must be fulfilled.

Due to the great thickness of the piston we assume that condition (2.6) is fulfilled also along AB .

3. Discretization of the region

The region, occupied by the material initially is discretized into a final number of elements by means of straight lines, parallel to the coordinate axes. As the material in a considerable distance in front of the piston moves as a rigid body during the forming process and the velocities are directed to the Oz axis, it is advisable to assume the length BC shorter than the real one. This leads to economy of computing time and memory. As the finite element nodes in TFARM [3,10] move during the deformation process like material points, the free boundary DF moves forward with the motion of the piston, e. g. the material starts to flow out of the opening. During that motion the element at point D , which is a singular point, deforms considerably. As soon as point E moves along the Oz axis at a distance of the order of the finite-element sides, a new mesh is built, which is the same as the initial one in the region $ABCDE$, but has a new column in front of the opening DE . The deformed and degenerated mesh around point D is now corrected. As the length BC is chosen shorter than the real one, e. g. the piston is far beyond the side AB , we assume the new region to have the same length BC as the previous one. In this way the piston is far beyond the opening DE during the whole time of the process. The values of the effective strain $\bar{\epsilon}$, the effective strain-rate $\bar{\dot{\epsilon}}$, and of the temperature T are transferred from the old to the new mesh [3]. As soon as the piston covers a distance, causing flow of the material of the order of the side of the finite element, the initial regular mesh is built again, applying a second column of elements at the opening etc. As soon as the length DF becomes sufficiently large, the material at a certain distance in front of DE moves as a rigid body and the velocities have the Oz direction. This makes possible to stop adding new columns of elements and the new regular meshes remain always the same. Then conditions (2.2)₁ and (2.6) are fulfilled at the boundary FE' .

Using one and the same regular mesh in the region $ABCDE$ at certain time intervals enables to estimate the change of the different mechanical variables obtained by TFARM at certain space points. In this way the initiation, the place and the movement of plastic localization bands may be investigated.

4. Numerical solution

The method mentioned above was applied to solve the unsteady coupled thermomechanical process of axisymmetric extrusion of aluminium. The material characteristics, according to [11] are as follows:

Yield limit:

$$(4.1) \quad \sigma_p = L_0 \left(\frac{T_m}{T} \right)^{L_1} + L_2 \{ [1 - \exp(-L_3 \bar{\dot{\epsilon}}^{L_4})] [1 - \exp(-L_5 \bar{\epsilon})] \\ \times \left(\frac{T_m}{T} \right)^{L_6} - L_7 \bar{\epsilon} \bar{\dot{\epsilon}}^{L_8} [\text{arc tg}(\bar{\epsilon} - 3,5) + 1,45] \},$$

where $T_m = 523 \text{ K}$ and the values of L_i , $i = 0, 1, 2, \dots, 8$ are given in table 1.

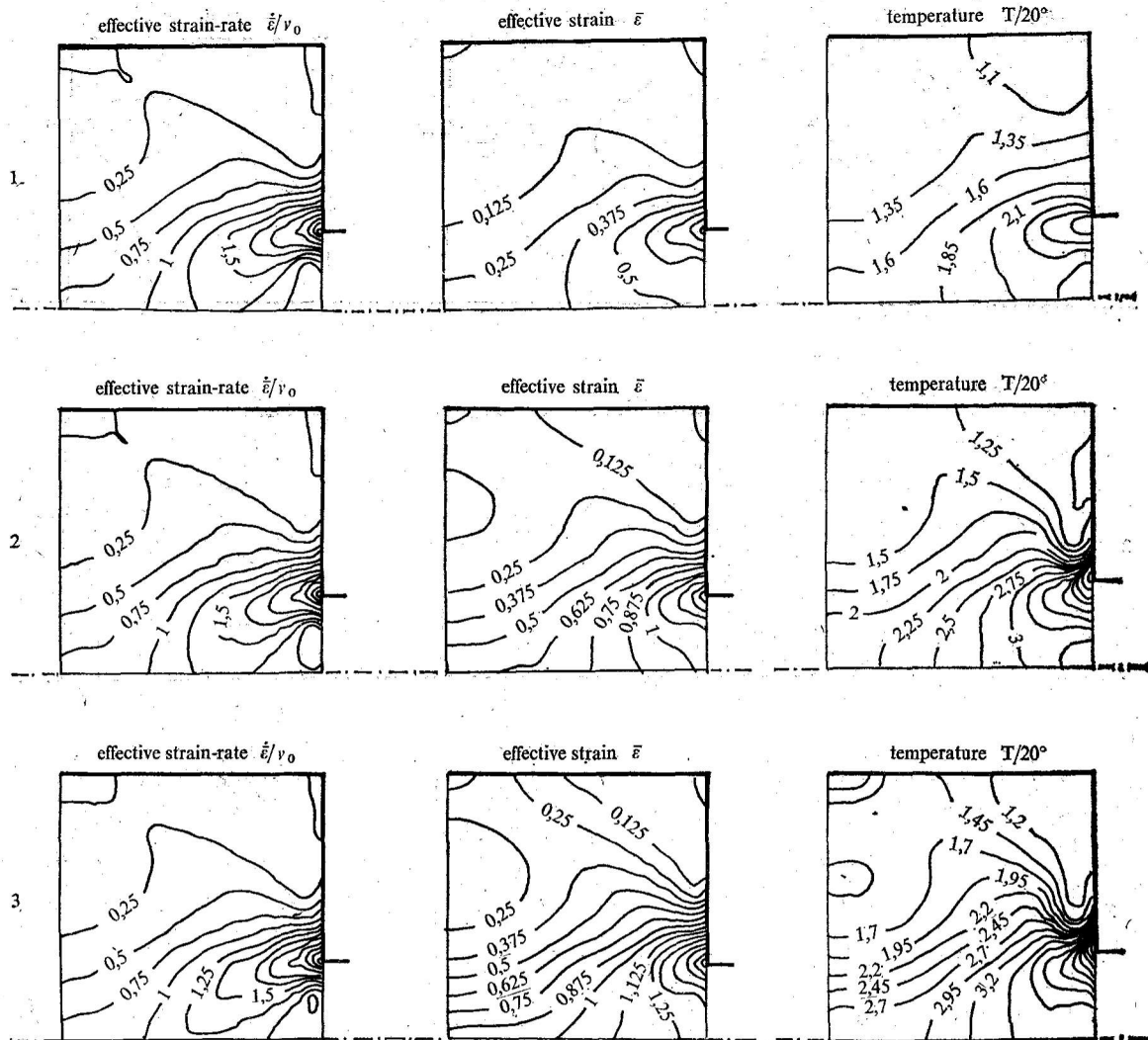


Fig. 2. a — effective strain-rate $\bar{\dot{\epsilon}}/v_0$
 b — effective strain $\bar{\epsilon}$
 c — temperature $T/20^\circ$
 1 — $\Delta h = 4$ mm, 2 — $\Delta h = 8$ mm, 3 — $\Delta h = 12$ mm $|\epsilon| = 0.84$

Heat conductivity coefficient:

$$(4.2) \quad \lambda = \lambda_0 + \lambda_t T,$$

where $\lambda_0 = 238,4$ J/(m. deg. s), $\lambda_t = 0$,

Specific heat supply:

$$(4.3) \quad c = c_0 + c_t T,$$

where $c_0 = 0,932$ J/(deg. g), $c_t = 0$,

Material density:

$$(4.4) \quad \rho = \text{const} = 2,71 \cdot 10^6 \text{ g/m}^3$$

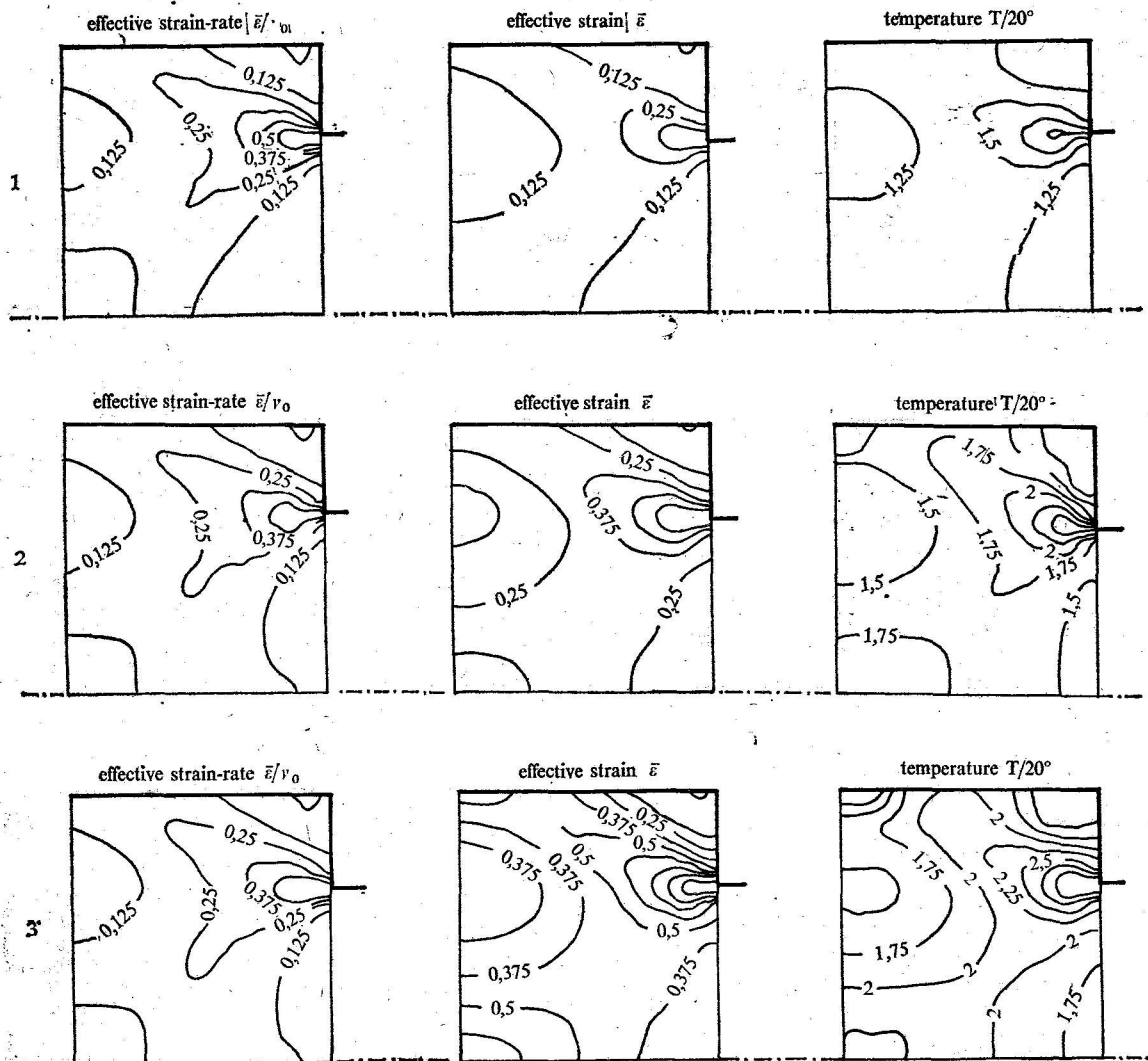


Fig. 3. a — effective strain-rate $\bar{\epsilon}/v_0$
 b — effective strain $\bar{\epsilon}$
 c — temperature $T/20^\circ$
 1 — $\Delta h = 7$ mm, 2 — $\Delta h = 14$ mm, 3 — $\Delta h = 21$ mm $|\epsilon| = 0,51$

The coefficient, determining what portion of the strain-rate energy turns into heat:
 (4.5)
$$\psi = 0,95.$$

According to the method, given in [11], the following values of H were calculated:

(4.6)

BC:	$H = 27,86 \text{ J}/(\text{m}^2 \cdot \text{deg. s})$
CD:	$H = 58,49 \text{ J}/(\text{m}^2 \cdot \text{deg. s})$
DE, DF and FE':	$H = 228,00 \text{ J}/(\text{m}^2 \cdot \text{deg. s}).$

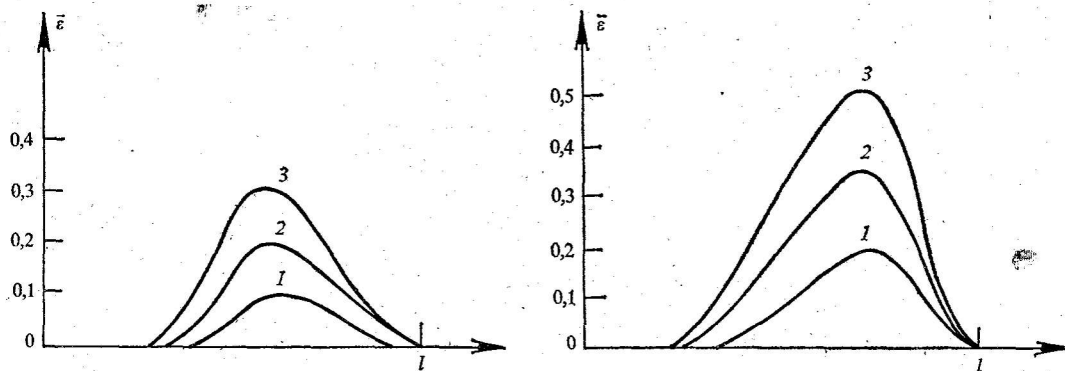


Fig. 4. a — effective strain $\bar{\epsilon}$ at $|\epsilon| = 0,84$ and $r = 8,5$ mm
 b — effective strain $\bar{\epsilon}$ at $|\epsilon| = 0,51$ and $r = 8,5$ mm

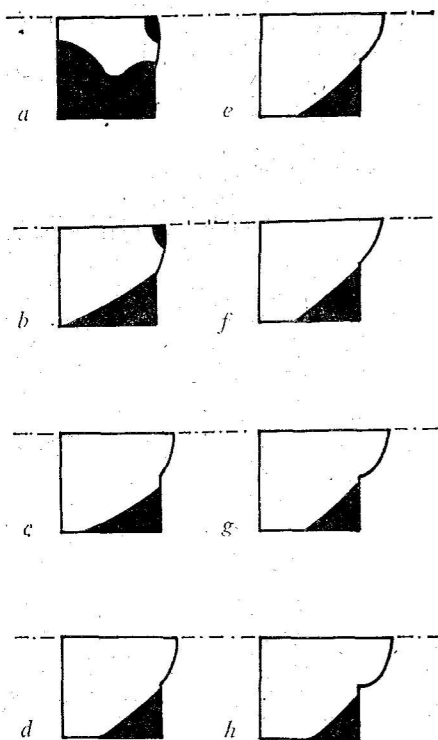


Fig. 5 Plastic zone development at $|\epsilon| = 0,84$
 ■ — rigid, □ — plastic

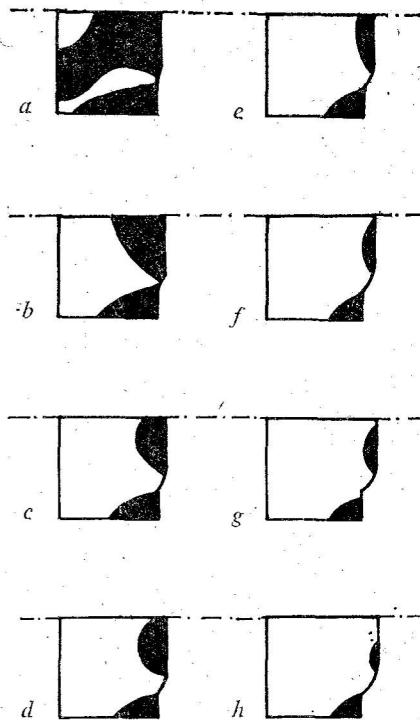


Fig. 6 Plastic zone development at $|\epsilon| = 0,51$
 ■ — rigid, □ — plastic

The boundary conditions are:
 Temperature of the surroundings

(4.7) $T_{ref} = \text{const} = 20^\circ\text{C}.$

Piston velocity:

(4.8) $v_0 = 0,001$ m/s.

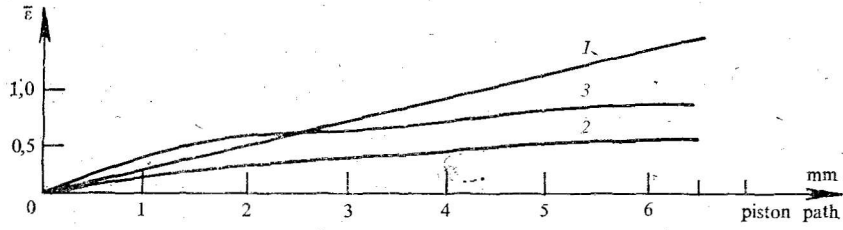


Fig. 7 Effective strain $\bar{\epsilon}$
 1 — at the localization band
 2 — below the localization band
 3 — above the localization band

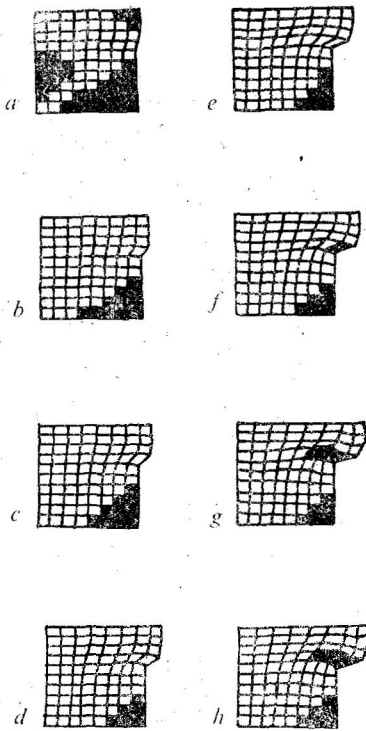


Fig. 8. ■ — region of fulfilled conditions for plastic localization at $|\epsilon| = 0,48$

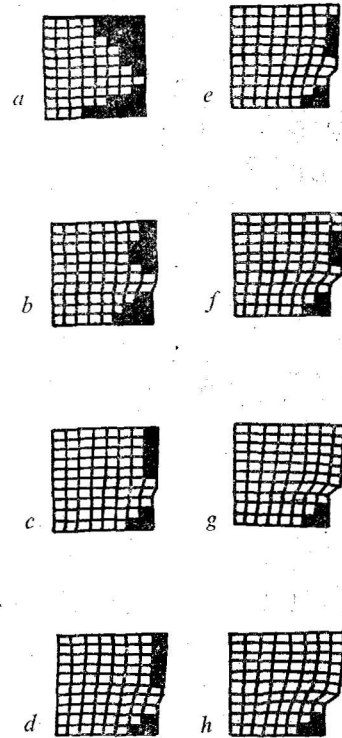


Fig. 9. ■ — region of fulfilled conditions for plastic localization at $|\epsilon| = 0,51$

Initial temperature distribution:

$$(4.9) \quad T(r, z, 0) = \text{const} = 20^\circ\text{C}.$$

The problem was solved for two values of the reduction ratio $|\epsilon|$. Fig. 2 and 3 show the distribution of temperature T , effective strain-rate $\dot{\epsilon}$ and effective strain $\bar{\epsilon}$ at $|\epsilon| = 0,84$ and $|\epsilon| = 0,51$, corresponding to $R_1 = 10$ mm and $R_2 = 4$ and 7 mm, at different piston paths Δh . The figures show that the high strain concentration near the opening causes a high temperature increase there. A band of higher temperature and effective strain values is observed beyond the boundary CD . The rapidly growing pick in Fig. 4 shows that a plastic localization band is formed there. This band moves

at the beginning of the process and takes soon a steady position. The plastic zone changes at the beginning too and becomes soon steady (Fig. 5 and 6). This phenomenon may be explained by the change of the material properties with the increasing temperature during the deformational process. Figure 7 shows the change of the effective strain during the piston movement at three points of the region — on the localization line, below it and above it. It is seen, that the deformation outside the localization band becomes steady, since on the line it grows continuously and tends to infinity.

Calculations were made at different piston velocities v_0 . This velocity has no influence on the dead zones. It has an influence on the temperature distribution. The temperature pick is much more expressed at higher velocities v_0 .

The fulfilment of the conditions for initiation of plastic localization bands was proved [12]. Figures 8 and 9 show the regions where plastic localization may take place. The comparison with figures 5 and 6 show that these are the regions between the plastic and the dead zones.

5. Conclusions

The numerical investigation of the extrusion process shows that plastic localization depends at the beginning on the piston path. Due to the coupling of the thermal and the deformational processes, and their unsteady character, the plastic localization band, built at the beginning moves and reaches later a stable position. The sensitivity of the process to the developed temperature is considerable and should not be neglected.

Acknowledgement.

The present investigation was carried out during the stay of the author at the Lehrstuhl A für Mechanik, Technische Universität München, under the fellowship of the Alexander-von-Humboldt Association. Part of it was supported by the Bulgarian Committee of Science. The author is highly indebted to the institutions mentioned above, as well as to Prof. Dr. h. c. H. Lippmann and to Dr. N. L. Dung for the numerous interesting and useful discussions. Numerical calculations were carried out by means of the program system TFARM, belonging to the TU Munic, TU Hamburg-Harburg and the Bulgarian Academy of Sciences.

References

1. Lippmann, H. *Mechanik des plastischen Fließens*. — Berlin, Springer Verlag 1981.
2. Cheng, J. H. Automatic Adaptive Remeshing for Finite Element Simulation of Forming Processes. — *Int. J. Numer. Meth. Eng.*, 20, 1988, 1-18.
3. Erlmann, K., N. L. Dung. Berechnung der Metallumformung mit der Finite-Element-Methode — *Forsch. Ing.-Wes.*, 46, No 3, 69-104, 1980.
4. Zienkiewicz, O. C., P. C. Jain, E. Onate. Flow of Solids during Forming and Extrusion. — *Some Aspects of Numerical Solutions*, *Int. J. Solids Structures*, 14, 1978, 15-38.
5. Argyris, J. H., J. St. Doltinis. On the Natural Formulation and Analysis of Large Deformation Coupled Thermomechanical Problems. — *Computer Methods in Appl. Mech. and Eng.*, 25, 1981, 195-253, North. Holand Publ. Co.
6. Zienkiewicz, O. C., E. Onate, J. C. Heinrich. A General Formulation for Coupled Thermal Flow of Metals Using Finite Elements. — *Int. J. Numer. Methods Eng.*, 17, 1981, 1497-1514.
7. Teodosiu, Cr. Thermomechanical Coupling during Hot Working Processes. — *Thermomechanical Coupling in Solids*, Bui H. D., R. S. Nguen (Ed.), Elsevier Science Publishers B. V. (North-Holand) IUTAM, 1987, 343-357.
8. Teodosiu, Cr., I. Rosu, T. Dumitrescu. Upper-Bound Analysis of Hot Extrusion of Axisymmetric Rods and Tubes, *Mécanique Appliquée*, 28, 1983, 3, 317-341.
9. Chenot, J. L., L. Felgeres, B. Lavarenue, J. Salencon. A Numerical Application of the Slip Line Field Method to Extrusion through Conical Dies. — *Int. J. Eng. Sci.*, 16, 1978, 263-273.
10. Bontcheva, N. A Method for Simulating of Nonstationary Thermoplastic Processes. — *Theoretical and Appl. Mech.* (in print).
11. Becker, K., H. Lippman, E. Teubl. Plastic Behaviour of Metals and Strain Localization, *Naturwissenschaften*, 72, 1985, 633-634.
12. Bontcheva, N., A. Baltov, St. Todorov, M. Pesheva. Plastic localization band at non-homogeneous plane strain and coupled thermo-plastic processes. — *Theoretical and Applied Mechanics* (in print).

Received 2. 06. 1988.